

Failure of brittle adhesive joints

Z Suo

Department of Mechanical Engineering, University of California, Santa Barbara, CA 93106.

Several mechanics problems of brittle adhesive joints are discussed in the light of recent calculations, including issues in fracture testing, concept of nominal toughness, configurational stability of mode-I in-layer fracture, tunnel crack and parallel debond due to residual stresses.

Notation

- α_a, α_s thermal expansion coefficients (substrate, adhesive)
 ν_a, ν_s Poisson's ratios (substrate, adhesive)
 E_a, E_s Young's modulus (substrate, adhesive)
 μ_a, μ_s shear modulus (substrate, adhesive)
 α, β Dundurs parameters ($\alpha > 0$ means adhesive is compliant compared with substrate)

$$\alpha = \frac{(1 - \nu_a)/\mu_a - (1 - \nu_s)/\mu_s}{(1 - \nu_a)/\mu_a + (1 - \nu_s)/\mu_s}$$

$$\beta = \frac{1}{2} \frac{(1 - 2\nu_a)/\mu_a - (1 - 2\nu_s)/\mu_s}{(1 - \nu_a)/\mu_a + (1 - \nu_s)/\mu_s}$$

- ε oscillation index for interfacial cracks

$$\varepsilon = \frac{1}{2\pi} \ln \frac{1 - \beta}{1 + \beta}$$

- σ magnitude of biaxial residual stress
 G energy release-rate
 G_c nominal fracture energy of adhesive joints
 G_{Ic} fracture energy of adhesive in bulk
 G_{ss} steady-state energy release rate for a tunnelling crack
 K_I, K_{II} local stress intensity factors
 $K_I^\infty, K_{II}^\infty$ remote stress intensity-factors
 K_{Ic} *in situ* toughness of adhesives
 K_{Ic}^∞ nominal mode-I toughness for adhesive joints
 t thickness of adhesive layers
 ΔT temperature difference from processing temperature to room temperature
 w width of each substrate for bend specimen
 M bending moment per unit thickness

Introduction

Polymeric adhesives have been used for many years to join component members. With the advent of new materials for high temperature applications, such as ceramic- and intermetallic-matrix composites, inorganic adhesives with load capacity at elevated temperatures are in increasing demand. One of the concerns is the substantial residual stresses developed in various joining techniques, which may cause failure even before any external load is applied. The problem area initially captured our attention for a rather different technical reason. In the course of

developing interfacial fracture mechanics to assess the role of interfaces and fibre coatings in ceramic-matrix composites, we found that various sandwich specimens are ideal for measuring interfacial fracture energy.

Several recent experimental observations and relevant fracture mechanics solutions are discussed here. It is envisioned that results developed in the context of adhesive joints may be applicable for other sandwich structures, such as laminates for structural or electronic applications, and coatings or reaction product layers in composites. Attention is limited to brittle adhesive joints so that elastic fracture mechanics is applicable. Adhesive layers are assumed to be very thin compared with substrates.

Fracture Tests

Many conventional fracture specimens have been used to test adhesive joints. The bend geometry in Fig. 1a is taken as an illustration (Cao and Evans 1989). The sandwich is made by joining two identical substrates with a thin adhesive layer. The top substrate is notched and two pre-cracks are introduced along the adhesive. Bend the joint up to the onset of the crack growth, and record the critical moment per unit thickness M .

Being very thin compared with the overall specimen dimension, an adhesive layer is frequently regarded as an easy fracture path in a base specimen which is otherwise homogeneous. The critical load such as the moment M is usually converted to fracture toughness according to the elasticity solution for the *homogeneous* base specimen. Fracture toughness can be represented either by the mixed-mode stress-intensity factors, or by the energy release-rate and the loading phase. Calibrations are available for many experimentally feasible geometries. For the bend specimen of Fig. 1a, the mixed-mode stress-intensity factors are (e.g., Suo 1990)

$$K_I^\infty = \sqrt{3} M w^{-3/2}, \quad K_{II}^\infty = 1.5 M w^{-3/2} \quad (1)$$

and the energy release rate and loading phase $\psi = \tan^{-1}(K_{II}^\infty / K_I^\infty)$

$$G = \frac{21}{4} \left(\frac{1 - \nu_s^2}{E_s} \right) \frac{M^2}{w^3}, \quad \psi = \tan^{-1} \left(\frac{\sqrt{3}}{2} \right) \approx 41^\circ \quad (2)$$

At such a macroscopic level (Fig. 1b), all damage processes at the scale of the layer thickness or below is collectively parameterized by the *nominal fracture toughness*. This evaluation approach has been used in the adhesion community for many years, and the rationale behind it is analogous to that of the small-scale-yielding in ductile fracture mechanics (Hutchinson 1983).

At a higher magnification, one sees details on the order of the adhesive thickness and may therefore appreciate how they affect the nominal fracture toughness. Residual stress microcracks perpendicular to the interfaces may exist in the layer prior to testing, for example, which are found to reduce the nominal fracture toughness (Zdaniewski, *et al* 1987). Upon loading the primary pre-cracks have been observed to propagate in a variety of ways, including straight or wavy paths within the layer, paths along one of the interfaces, and paths alternating from interface to interface through the layer. The nominal toughness depends on these details and many others (*e.g.*, Chai 1988, Oh, *et al.* 1988, Pabst and Elssner 1980).

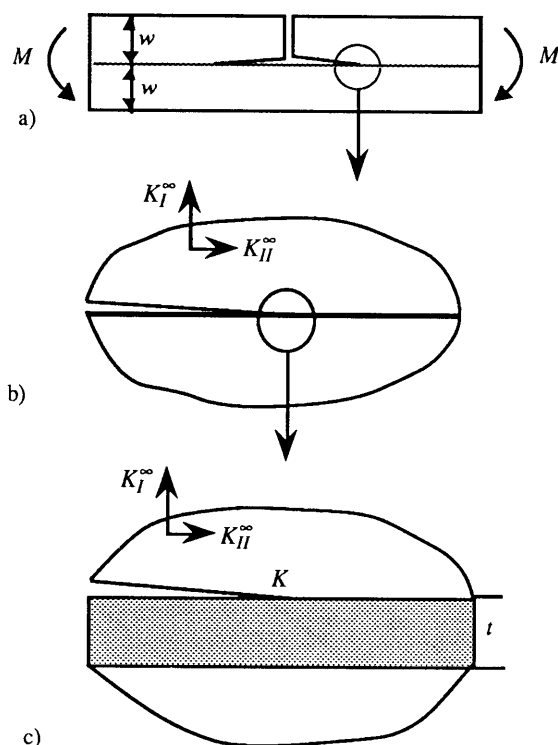


FIG. 1. Fracture test of an adhesive joint viewed at increasing magnifications. a) A bend specimen, M being moment per unit thickness. b) Nominal crack tip field treating the adhesive as an easy fracture path in an otherwise homogeneous sample. c) An interfacial crack tip and the far field loads.

Nominal Fracture Toughness

Two idealized situations can be understood readily: i) a flat crack running within the adhesive layer, and ii) debonding along an adhesive-substrate interface. If the near-tip damage-zone for each situation is confined within a region much smaller than the adhesive thickness, as a consequence of the conservation of the Rice's J -integral, the measured nominal fracture energy G_c equals the energy actually released at the crack tip. The value of the nominal G_c is the *in situ* fracture energy G_{Ic} for the bulk adhesive if a mode-I path can be found in it, or the mixed-mode interface fracture energy if the crack propagates along the interface.

Notice that in the above the residual stress and the layer thickness do not affect the nominal fracture energy, because the residual stress induced strain energy is not released, as long as

the layer is thin and still remains adherent to one of the substrates in the wake. The possibility of parallel debonding will be discussed in a later section.

The above energetic considerations can be reinterpreted in terms of the stress-intensity factors.

With a mode-I specimen, such as a double-cantilever-beam, by symmetry a crack along the centerline in the adhesive is locally mode-I. The joint fractures when the local stress-intensity factor attains the toughness of the *in situ* bulk adhesive K_{Ic} . There is a simple connection between the nominal toughness K_{Ic}^∞ and the bulk adhesive toughness K_{Ic} (*e.g.*, Fleck, Hutchinson and Suo 1990)

$$K_{Ic}^\infty = \left(\frac{1 + \alpha}{1 - \alpha} \right)^{1/2} K_{Ic} \quad (3)$$

where α is one of the Dundurs parameters characterizing the relative stiffness of the two materials. Adhesives are usually compliant compared with substrates ($\alpha > 0$), so that the apparent toughness is higher than the toughness of the bulk adhesive. More intuitively, the mechanical load to fracture a bulk adhesive is much lower than that to fracture the same adhesive sandwiched between stiffer substrates. Such an effect is due entirely to the elastic mismatch of the two solids and may be referred to as a *stress-intensity shielding* effect.

If the crack runs along an interface (Fig. 1c), interfacial fracture mechanics (*e.g.*, Rice 1988) may be used. When the layer is thin, a connection between the interfacial stress-intensity factor K (a complex quantity) and the remote stress-intensity factors exists

$$K = (1 - \alpha)^{1/2} \cosh \pi \epsilon \left(K_I^\infty + i K_{II}^\infty \right) t^{-i\epsilon} \exp(i\omega) \quad (4)$$

where $i = \sqrt{-1}$, ω is an angle dependent on the Dundurs parameters and available in Suo and Hutchinson (1989). Equation (4) is universal in that it is independent of the joint geometry. For a given joint, K_I^∞ and K_{II}^∞ relate to the applied loads by the calibration of type (1) appropriate for the homogeneous base specimen. The sandwich setup has recently been exploited to measure interfacial fracture energy (Cao and Evans 1989, Wang and Suo 1990).

Configurational Stability of the Mode-I in-Layer Fracture

A model fracture test was carried out recently with a brittle compliant layer sandwiched in stiff substrates (Wang and Suo 1990). When the remote load was predominantly mode-I, cracks were observed to run within the layer rather than along the interfaces. The in-layer fracture was thought abnormal since the fracture energy for the adhesive was more than twice of that for the interfaces for the particular system. The in-layer fracture was found configurationally stable even with some proportion of mode-II load (up to roughly 8% of the mode-I load). When a significant amount of mode-II is applied the fracture path was observed along one of the interfaces. As a consequence of the different fracture paths selected for different loading phases, a discontinuity was found on the nominal fracture energy vs. loading phase curve (Fig. 2).

The in-layer fracture and associated discontinuity in the mixed-mode fracture energy curve were also independently observed by Thouless (1990) in testing a brittle polymer sandwiched in glass double-cantilever-beams. The stability of the mode-I in-layer fracture is intriguing because, in homogeneous double-cantilever-beam specimens, the mode-I crack is well known to divert from the symmetry axis.

A quantitative fracture mechanics study has been carried out

recently by Fleck, Hutchinson and Suo (1990). The stability of the in-layer fracture is found to be consistent with the established T -stress criterion (Cotterell and Rice 1980), and is primarily accommodated by the large elastic mismatch between the adhesive and substrates and the nature of residual stress. Specifically, the mode-I in-layer fracture is favorable as opposed to the interfacial fracture when the adhesive is more compliant than the substrates, and the in-layer residual stress is compressive or slightly tensile.

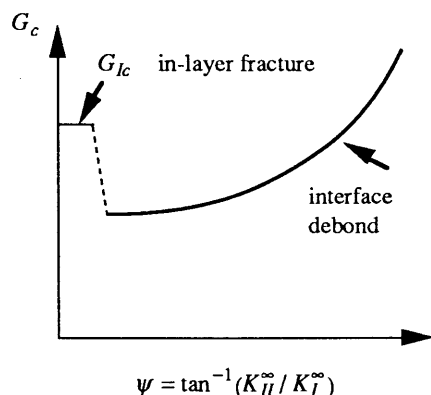


FIG. 2. Schematic of the observed nominal fracture energy vs. loading phase curve. The discontinuity is due to the different fracture paths selected for different loading phases.

Tunnelling Crack Formation

Biaxial residual stresses usually develop in adhesive layers during bonding processes. For inorganic adhesives, a major source of the residual stresses is thermal expansion mismatch, with the magnitude

$$\sigma = \frac{E_a}{1 - \nu_a} [(\alpha_a - \alpha_s) \Delta T] \quad (5)$$

The residual stress is tensile when the adhesive has larger thermal expansion coefficient than the substrates.

When an adhesive layer is under substantial residual tension, transverse cracks may form in the adhesive even before any external load is applied (e.g., Zdaniewski, *et al.* 1987). Similar cracks are observed in reaction product layers around fibres in some composites. Cracks may penetrate interfaces into substrates if the latter are brittle, as observed in a model system consisting of a sapphire layer between two glass blocks (Chiao and Clarke 1990). Debonding is also possible at the intersection of the interfaces and cracks.

As illustrated in Fig. 3, a crack initiates from an internal flaw and extends within the layer. Complications such as penetration and debond are ignored here. The tunnelling crack eventually reaches a steady-state: the entire front maintains the shape as it advances and the energy released per unit advance is no longer dependent on the tunnel length. An estimate of the energy release-rate for the *steady-state tunnelling* will therefore provide a design limit for the residual stress and layer thickness. The approach used below is attractive because it captures the actual three dimensional mechanism of the crack tunnelling as a feature, yet the calculation is based on two dimensional stress fields which can be analyzed as a plane strain elasticity problem. The calculation is independent of the unknown shape of the tunnel front.

At the steady-state the process of the entire tunnel front

advancing a unit distance is equivalent to removing a slice of uncracked material of unit thickness far ahead of the front and inserting a slice of material of a unit thickness with a crack far behind of the front. The net potential energy drop for this process is equal to that for creating a *through-crack* in the slice of material of unit thickness

$$\Delta U = \frac{1}{2} \sigma \int_{-t/2}^{+t/2} \delta(x) dx \quad (6)$$

where $\delta(x)$ is the crack opening displacement profile for the plane strain through-crack. On the other hand the steady-state energy release rate G_{ss} is a constant along the entire tunnelling front and equals the fracture energy G_{lc} of the adhesive. The potential energy loss should be balanced by the energy consumed in creating the new crack area

$$\Delta U = G_{ss} t \quad (7)$$

Comparing the above gives

$$G_{ss} = \frac{\sigma}{2t} \int_{-t/2}^{+t/2} \delta(x) dx \quad (8)$$

This equation is valid for adhesive and substrates with different elastic moduli. The only missing information is the displacement jump of a through-crack in a plane perpendicular to the interfaces, which has to be calculated numerically in general.

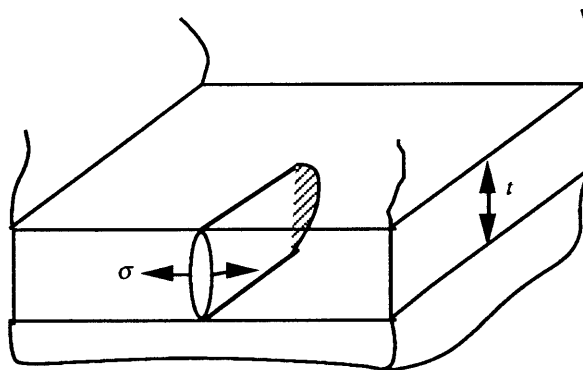


FIG. 3. A transverse steady-state tunnelling crack in an adhesive.

If the elastic constants of the substrates and adhesive are identical, the corresponding plane strain problem is a through-crack in a homogeneous plane (a Griffith crack) and the solution is readily available

$$\delta(x) = 4\sigma \frac{1 - \nu^2}{E} \sqrt{(t/2)^2 - x^2} \quad (9)$$

The integral (8) gives

$$G_{ss} = \frac{\pi}{4} \frac{1 - \nu^2}{E} \sigma^2 t \quad (10)$$

This final result may be interpreted in a variety of ways. For example, for given adhesive and substrate materials with fixed fracture energy G_{lc} and residual stress σ , the equation predicts the thickest adhesive layer one can make without long tunnel cracks. Analogous predictions for thin films have previously been made and confirmed experimentally (Hu and Evans 1989).

Parallel Debonding

When a sandwich layer is under substantial residual compression, debonding may take place along the *two*

interfaces. The phenomenon was observed in preparing Al_2O_3 -SiC- Al_2O_3 sandwiches (private communication with A.G. Evans). The sandwiches were diffusion bonded at an elevated temperature, but debonded into three pieces in the cool-down. Parallel debonding under uniaxial loads has been observed in laminates with center notches or matrix cracks (e.g., O'Brien 1987, Spearing, Beaumont and Ashby 1990).

It can be shown with the Eshelby cut-and-paste technique that, as far as the stress intensity is concerned, the residual compression is equivalent to a mechanical load of layer pull-out. Depicted in Fig. 4 is a slightly generalized situation in which an opening load represented by K_I^∞ is included, in addition to the pull-out stress σ . It is envisioned that the pull-out stress itself may not be high enough to trigger debonding, but the structure debonds with an additional remote mode-I load.

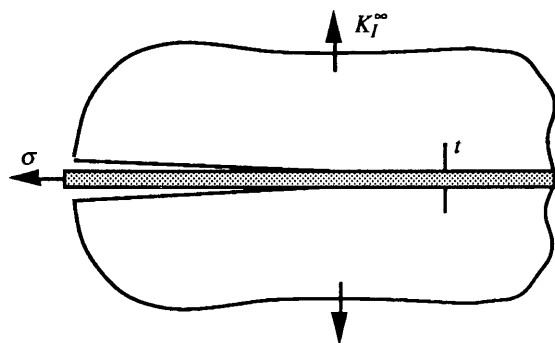


FIG. Parallel debonding due to residual compression and remote stress intensity.

To gain insight into this setup, we ignore the moduli difference in this preliminary treatment. By an energetic argument, one obtains the energy release rate at each tip under combined loads σ and K_I^∞

$$G = \frac{1-\nu^2}{E} \left(\frac{K_I^{\infty 2}}{2} + \frac{\sigma^2 t}{4} \right) \quad (11)$$

Hence the interfacial fracture energy G_c can be inferred if one measures σ and the critical K_{Ic}^∞ triggering debond. Taking $K_I^\infty = 0$ in (11) and comparing with (10), one finds the energy available to create a tunnel crack is π times of that to debond the two interfaces.

Recall the Irwin formula as applicable for each crack tip

$$G = \frac{1-\nu^2}{E} (K_I^2 + K_{II}^2) \quad (12)$$

where K_I and K_{II} are stress-intensity factors at the upper crack tip. Comparing the two energy release-rate expressions, and keeping the linearity of the elasticity problem in mind, one reaches

$$\begin{aligned} K_I &= \frac{1}{\sqrt{2}} K_I^\infty \cos \phi + \frac{1}{2} \sigma \sqrt{t} \sin \phi \\ K_{II} &= -\frac{1}{\sqrt{2}} K_I^\infty \sin \phi + \frac{1}{2} \sigma \sqrt{t} \cos \phi \end{aligned} \quad (13)$$

The angle ϕ has to be determined by solving the full elasticity problem. An integral equation approach is used and the solution is $\phi \approx 17.5^\circ$.

Consider the case when $K_I^\infty = 0$. The above solution indicates that the pull-out stress induces a significant amount of crack face opening, along with the predominant sliding. By contrast, residual tension equivalent to a push-in mechanical stress induces a negative K_I , suggesting that debonding will be a pure mode-II sliding against friction. Therefore parallel debonding will more likely take place for adhesives in residual compression than in tension, provided other conditions are the same.

In a standard fracture test with an adhesive joints under residual tension, a possible scenario is that a single crack may first propagate along one interface under remote K_I^∞ , leaving the stressed adhesive on the other substrate. The exposed adhesive, which is analogous to a thin film under tension, may peel off from the substrate and parallel debonding follows. The nominal toughness K_{Ic}^∞ is reduced by the presence of the residual stress with this mechanism.

Acknowledgements

Support was provided by the Office of Naval Research contract N00014-86-K-0753, and the College of Engineering, University of California at Santa Barbara.

References

- Cao, H.C. and Evans, A.G., (1989), An experimental study of fracture resistance of bimaterial interfaces, *Mechanics of Materials*, **7**, 295-305.
- Chai, H. (1988), Shear fracture, *Int. J. Fracture*, **37**, 137-159.
- Chiao, Y.-H. and Clarke, D.R. (1990), Residual stress induced fracture in glass-sapphire composites: planar geometry, *Acta Met* in press.
- Cotterell, B. and Rice, J.R. (1980), Slightly curved or kinked cracks, *Int. J. Fract.* **16**, 155-169.
- Fleck, N.A., Hutchinson, J.W. and Suo, Z. (1990), Crack path selection in brittle adhesive joints, Harvard University Report MECH-156.
- Hu, M.S. and Evans A.G. (1989), The cracking and decohesion of thin films on ductile substrates, *Acta Met.*, **37**, 917-925.
- Hutchinson, J.W. (1983), Fundamentals of the phenomenological theory of nonlinear fracture mechanics, *J. Appl. Mech.*, **50**, 1042-1051.
- O'Brien, T.K. (1987), Generic aspects of delamination in fatigue of composite materials, *J. Am. Helicopter Soc.*, **32**, 13-18.
- Oh, T.S., Rodel, J., Cannon, R.M. and Ritchie, R.O. (1988), Ceramic/metal interfacial crack growth: toughening by controlled microcracks and interfacial geometries, *Acta Met.* **36**, 2083-2093.
- Pabst, R.F. and Elssner, G.E. (1980), Adherence properties of metal-to-ceramic joints, *J. Mater. Sci.*, **15**, 188-196.
- Rice, J.R. (1988), Elastic fracture mechanics concepts for interfacial cracks, *J. Appl. Mech.*, **55**, 98-103.
- Spearing, S.M., Beaumont, P.W.R. and Ashby, M.F. (1990), Fatigue damage mechanics of notched graphite-epoxy laminates, to be published.
- Suo, Z. (1990), Delamination specimens for orthotropic materials, *J. Appl. Mech.*, in press.
- Suo, Z. and Hutchinson, J.W. (1989), Sandwich specimens for measuring interface crack toughness, *J. Mater. Sci. Engng.*, **A107**, 135-143.
- Thouless, M.D. (1990), Fracture of a model interface under mixed-mode loading, submitted for publication.
- Wang, J.-S. and Suo, Z. (1990), Experimental determination of interfacial toughness using Brazil-nut-sandwich, *Acta Met* in press.
- Zdaniwski, W.A., Conway, J.C. and Kirchner, H.P. (1987), Effect of joint thickness and residual stresses on the properties of ceramic adhesive joints: II, experimental results. *J. Am. Ceram. Soc.*, **70**, 104-109.